Elementary Steps in the Reaction Mechanism of Pyruvate Dehydrogenase Multienzyme Complex from *Escherichia coli*: Kinetics of Flavin Reduction†

Steven K. Akiyama and Gordon G. Hammes*

ABSTRACT: The reduction and oxidation of the flavin on the pyruvate dehydrogenase multienzyme complex from *Escherichia coli* have been studied in 0.02 M potassium phosphate, pH 7.0, at 4 °C by using spectroscopic and stopped-flow techniques. Absorbance and fluorescence titrations of the enzyme-bound flavin with NADH in the presence of NAD^+ indicate the ratio (reduced flavin)(NAD^+)/(oxidized flavin)(NADH) is $\sim 10^{-3}$. When the enzyme complex is mixed with thiamin pyrophosphate, Mg^{2+}, pyruvate, and CoA, the absorption spectrum is predominately that of the two-electron reduced flavin, and the fluorescence is quenched ~65%. Stopped-flow studies in which enzyme complex incubated with thiamin pyrophosphate and Mg^{2+} is mixed with thiamin pyrophosphate, Mg^{2+}, pyruvate, and CoA reveal that flavin reduction occurs via two first-order kinetic processes. The faster process, observed by monitoring fluorescence changes and absorbance changes at 530 nm, has a limiting rate constant of ~ 30 s^{-1} at high pyruvate concentrations. The slower process, observed by monitoring fluorescence changes or absorbance changes at 450 and 530 nm, has a limiting rate constant of 2.3–2.6 s^{-1} at high pyruvate concentrations. Only the faster process is sufficiently rapid to be of importance in the catalytic cycle, and the establishment of steady-state catalysis occurs in <50 ms. Both rate constants are strongly dependent on the pyruvate concentration but are not dependent on the CoA concentration as long as it is equal to or greater than the concentration of CoA–enzyme sites. The rate of the faster process and the rate of catalytic lipoic acid acetylation are increased by oxaloacetate. These results suggest that the rate-determining step in the overall reaction is in the formation of hydroxyethylthiamin pyrophosphate on pyruvate decarboxylase. If the enzyme complex is not preincubated with thiamin pyrophosphate, a slow conformational change associated with thiamin pyrophosphate binding can be rate limiting. The oxidation and reduction of flavin by NAD^+ and NADH, respectively, occur with a characteristic time constant of ≤20 μs. These results can be explained in terms of the rapid kinetic process being formation of the two-electron reduced enzyme and the slower process being partial conversion of the two-electron reduced enzyme to the four-electron reduced enzyme.

The pyruvate dehydrogenase multienzyme complex from *Escherichia coli* consists of a regular arrangement of three enzymes: pyruvate decarboxylase (E_1), dihydrolipoyl transacetylase (E_2), and dihydrolipoyl dehydrogenase (E_3) which are found in the complex with a polypeptide chain ratio 24:24:12 (Koike et al., 1963; Willms et al., 1967; Angelides et al., 1979). These enzymes are noncovalently bonded to form an aggregate with a molecular weight of 4.8×10^6 (Reed, 1974; Angelides et al., 1979), which catalyzes the decarboxylation of pyruvic acid and the acetylation of CoA[1] through the series of reactions (Koike & Reed, 1960)

$$\text{pyruvate} + E_1[\text{TPP}] \rightarrow CO_2 + E_1[\text{hydroxyethyl-TPP}] \quad (1)$$

$$E_1[\text{hydroxyethyl-TPP}] + E_2[\text{Lip-S}_2] \rightleftharpoons E_1[\text{TPP}] + E_2[\text{HS-Lip-S-acetyl}] \quad (2)$$

$$E_2[\text{HS-Lip-S-acetyl}] + \text{CoA} \rightleftharpoons E_2[\text{Lip-(SH)}_2] + \text{acetyl-CoA} \quad (3)$$

$$E_2[\text{Lip-(SH)}_2] + E_3[\text{FAD}] \rightleftharpoons E_2[\text{Lip-S}_2] + E_3[\text{FAD(red)}] \quad (4)$$

$$E_3[\text{FAD(red)}] + NAD^+ \rightleftharpoons E_3[\text{FAD}] + \text{NADH} + H^+ \quad (5)$$

where TPP, Lip-S_2, and Lip-(SH)_2 are thiamin pyrophosphate and oxidized and reduced lipoic acid, respectively. The brackets denote cofactors and intermediates which are tightly or covalently bound to the enzyme.

This mechanism requires lipoic acid residues to interact with the catalytic sites on all three enzymes. Although resonance energy transfer measurements suggest that the catalytic sites are too far apart to be bridged by a single lipoic acid (Shepherd & Hammes, 1976, 1977), the lipoic acid residues are close to each other (Angelides & Hammes, 1979) and interlipoic acid transfers of acetyl groups can occur (Brown & Perham, 1976; Bates et al., 1977; Collins & Reed, 1977). Forty-eight lipoic acids per molecule of complex can be acetylated by pyruvate via eq 1 and 2 (Speckhard et al., 1977). The results of quenched-flow experiments indicate acetylation at 4 °C and pH 7.0 occurs by two pathways with only the faster one having a sufficiently rapid rate to be catalytically significant (Akiyama & Hammes, 1980). The rate constant of the faster process reaches a limiting value of 45–60 s^{-1} at high pyruvate concentrations, the exact value depending on the specific mechanism assumed. About half of the lipoic acids are acetylated by the faster process. Deacetylation by CoA on the catalytic pathway occurs at a much faster rate than acetylation.

In this work the reduction of the flavin by the addition of pyruvate and CoA to the enzyme complex incubated with thiamin pyrophosphate and Mg^{2+} was examined by fluorescence and absorbance measurements at 4 °C and pH 7.0. Stopped-flow measurements of fluorescence quenching indicate two first-order processes occur. The faster process has a limiting rate constant of 30 s^{-1} and the slower process a limiting rate constant of 2.6 s^{-1} at high pyruvate concentrations. When changes in flavin absorbance are monitored at 450 nm, only the slower process is observed, while both processes are observed at 530 nm. Although CoA is required for these reactions to occur, the rate constants are not dependent on the concentration of CoA if it is greater than that of the enzyme

† From the Department of Chemistry, Cornell University, Ithaca, New York 14853. *Received June 17, 1980.* This work was supported by grants from the National Institutes of Health (GM 13292) and the National Science Foundation (PCM77-11392). S.K.A. is a National Institutes of Health Predoctoral Trainee (GM 00834 and GM 07273).

[1] Abbreviations used: CoA, coenzyme A; NAD, nicotinamide adenine dinucleotide; NADH, reduced NAD; FAD, flavin adenine dinucleotide.

0006-2960/81/0420-1491$01.25/0

complex. Oxidation and reduction of the flavin by NAD^+ and NADH occur with a characteristic time constant of ≤ 20 μs. A mechanism is suggested in which the faster process corresponds to formation of the catalytically active two-electron reduced enzyme, while the slower process corresponds to subsequent partial conversion to the catalytically inactive four-electron reduced enzyme.

Experimental Procedures

Materials. The thiamin pyrophosphate, sodium pyruvate, CoA, dithiothreitol, NAD^+ (grade V), NADH, oxaloacetate, and bovine serum albumin were obtained from Sigma Chemical Co., and enzyme grade ammonium sulfate was from Schwarz/Mann. The [3-^{14}C]pyruvate (15–25 Ci/mol) was obtained from New England Nuclear. It was dissolved in 0.02 M potassium phosphate, pH 7.0, to yield a stock solution of 250 μCi/mL which was stored at −10 °C and used within 4 days. The concentration of the stock solution was determined by the lactate dehydrogenase assay (Meister, 1950). All other chemicals were the best available commercial grades. All kinetic experiments and spectral measurements were carried out in a standard buffer of 0.02 M potassium phosphate, pH 7.0, at 4 °C. The buffer was deaerated by heating to boiling, cooling, and bubbling argon through it. All solutions were prepared with deionized, distilled water.

Pyruvate Dehydrogenase Complex. The pyruvate dehydrogenase complex was prepared from frozen *E. coli* cell paste (strain B, late log harvest, Miles Laboratories) by the method of Reed & Willms (1966). An ammonium sulfate precipitation (0.225 g of ammonium sulfate/mL) was used to separate the pyruvate dehydrogenase complex from the α-ketoglutarate dehydrogenase complex. At least 98% of the bound thiamin pyrophosphate was removed by dialyzing the enzyme against 0.1 M potassium phosphate, pH 8.25, and 3 mM ethylenediaminetetraacetic acid for 8 h at 4 °C (Shepherd & Hammes, 1976) followed by dialysis against 0.02 M potassium phosphate, pH 7.0, before use. The specific activity of the pyruvate dehydrogenase complex, as measured by the formation of NADH under standard conditions (Akiyama & Hammes, 1980), was between 25 and 40 μmol of NADH formed min^{-1} (mg of protein)$^{-1}$. The purity of the enzyme complex was checked by sodium dodecyl sulfate–polyacrylamide gel electrophoresis (Shepherd & Hammes, 1977). When necessary, the complex was further purified by an isoelectric precipitation at pH 4.9 (Reed & Willms, 1966). The protein concentration was determined by the method of Lowry et al. (1951) using bovine serum albumin as a standard with a correction factor of 0.93 and a molecular weight of 4.8×10^6 (Angelides et al., 1979).

Stopped-Flow Experiments. The stopped-flow experiments were done on a modified Durrum-Gibson stopped-flow spectrophotometer (Dionex Corp.) thermostated at 4 °C. The delivery syringe barrels were made out of 0.286-in. True-bore tubing (Ace Glass, No. 8700-45) and equipped with Hamilton No. 1002 plungers. The light source was either a 50-W tungsten lamp (Osram No. 64610) or a 200-W xenon–mercury arc lamp (Canrad-Hanovia). In the fluorescence experiments a 460-nm cutoff filter (Corning) was inserted in front of the photomultiplier tube. The dead time of the instrument was determined to be 4–5 ms. Enzyme complex solutions for kinetic measurements were prepared by transferring concentrated stock enzyme complex (15–30 mg/mL) into the standard buffer alone or standard buffer with 4 mM thiamin pyrophosphate and 2 mM $MgSO_4$ and then equilibrating the enzyme on ice for 10–90 min. The ligand solutions, consisting usually of thiamin pyrophosphate, $MgSO_4$, pyruvate, CoA, and dithiothreitol in the standard buffer, were prepared so that no dilution of the thiamin pyrophosphate or $MgSO_4$ in the enzyme complex solution occurred upon mixing. In a stopped-flow experiment 0.15 mL each of the enzyme complex and ligand solutions was mixed. Each time course was transferred through a transient recorder (Biomation Model 802) to a PDP-11 computer (Digital Equipment Corp.) for processing and storage on discs.

Quenched-Flow Experiments. The combined quenched-flow (Lymn & Taylor, 1970) and pulsed quenched-flow apparatus (Fersht & Jakes, 1975) and the experimental protocol used to follow the time course of acetylation of the enzyme complex by [3-^{14}C]pyruvate have been previously described (Akiyama & Hammes, 1980; Akiyama, 1981). The enzyme complex solutions were prepared in the standard buffer with 4 mM thiamin pyrophosphate and 2 mM $MgSO_4$ in the same manner as for the stopped-flow experiments. The [3-^{14}C]pyruvate was diluted with nonradioactive pyruvate and dissolved in the same buffer. The final concentration of pyruvate was determined by mixing the pyruvate solutions with 1.5 mg of pyruvate dehydrogenase complex and assuming 10 nmol of pyruvate/mg of enzyme complex is covalently bound (Akiyama & Hammes, 1980). The final specific activities of the pyruvate solutions were $\sim 10^7$ cpm/μmol.

Temperature-Jump Experiments. The temperature-jump apparatus with fluorescence detection has been previously described (del Rosario, 1970). The excitation wavelength was 450 nm, and a 460-nm cutoff filter was used for viewing the emission. A temperature jump of 8 °C was applied to the sample thermostated at 8 °C. Samples were prepared by diluting the concentrated enzyme which had been dialyzed overnight against 0.1 M phosphate into 3 mL of 6.4 mM NAD^+ and 0.1 M potassium phosphate (pH 7.0) plus NADH stock solution. The sample was equilibrated in the apparatus 5–10 min before the first temperature jump and 1–5 min after mixing with fresh solution following each subsequent jump. The enzyme complex was able to undergo 30 temperature jumps over the course of 2 h without any significant loss of specific activity.

Steady-State Fluorescence and Absorbance Measurements. Fluorescence and absorbance spectra were measured with a Hitachi Perkin-Elmer MPF-3 spectrofluorometer and a Cary 118 spectrophotometer, respectively. In both cases the cell compartments were themostated at 4 °C and purged with argon.

Data Analysis. The amplitudes and rate constants for the stopped-flow experiments were calculated on a PDP-11 computer (Hilborn, 1972; Hilborn et al., 1973). Each rate constant represents an average obtained from 1–10 oscilloscope traces. The concentration dependences of the rate constants and the time course of acetylation by [3-^{14}C]pyruvate were fit to specified equations by using a nonlinear least-squares analysis.

Results

The equilibrium constant (eq 6) was determined by titrating

$$K_{eq} = \frac{(E_3[FAD])(NADH)}{(E_3[FAD(red)])(NAD^+)} \qquad (6)$$

the enzyme complex with NADH in the standard buffer at 4 °C in the presence of a constant amount of NAD^+. The ratio of flavin in the oxidized and reduced forms was determined from the absorption at 450 nm or the fluorescence emission at 520 nm (450-nm excitation). The characteristic absorbance and fluorescence of the reduced form were determined by extrapolation to infinite NADH concentration.

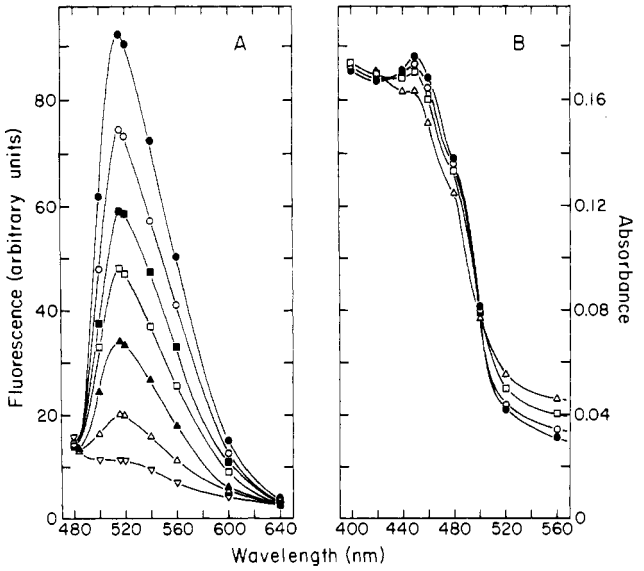

FIGURE 1: (A) Uncorrected fluorescence emission spectra (450-nm excitation, 8-nm bandwidth) of 0.13 μM pyruvate dehydrogenase complex (1.56 μM enzyme–flavin) at 4 °C and pH 7.0 in (●) 9.0 mM NAD^+ and 0.02 M potassium phosphate; plus NADH, (○) 3.7 μM, (■) 7.5 μM, (□) 11.2 μM, (▲) 22.5 μM, (△) 52.3 μM, and (▽) 144.5 μM. (B) Absorption spectra of 0.91 μM pyruvate dehydrogenase complex (10.9 μM enzyme–flavin) at 4 °C and pH 7.0 in (●) 7.8 mM NAD^+ and 0.02 M potassium phosphate; plus NADH, (○) 8.6 μM, (□) 17.2 μM, and (△) 47.0 μM.

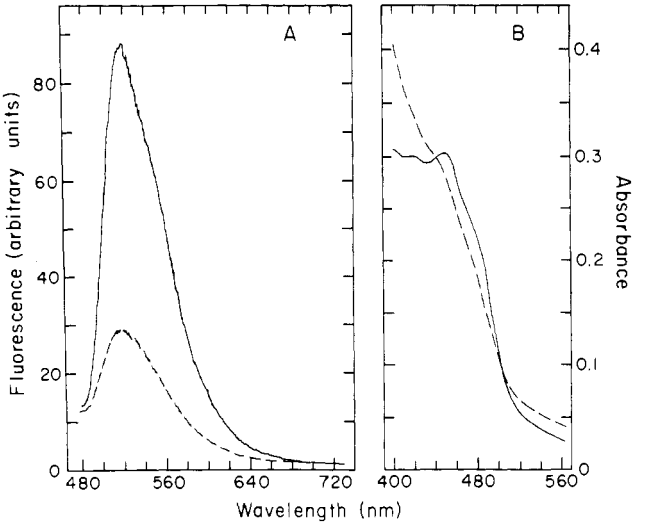

FIGURE 2: (A) Uncorrected fluorescence spectra (450-nm excitation, 6-nm bandwidth) of 0.19 μM pyruvate dehydrogenase complex (2.28 μM enzyme–flavin) at 4 °C and pH 7.0 in (—) 4 mM thiamin pyrophosphate, 2 mM $MgSO_4$, and 0.02 M potassium phosphate, pH 7.0, (– – –) plus 5 mM pyruvate, 0.5 mM CoA, and 2 mM dithiothreitol. (B) Absorption spectra of 1.8 μM pyruvate dehydrogenase complex (21.6 μM enzyme–flavin) at 4 °C and pH 7.0 and (—) 0.02 M potassium phosphate, (– – –) plus 4 mM thiamin pyrophosphate, 2 mM $MgSO_4$, 4 mM pyruvate, 0.3 mM CoA, and 3 mM dithiothreitol.

The concentrations of NAD^+ and NADH were corrected for the amount of reduced flavin formed. Representative titration data are presented in Figure 1. In the fluorescence titration the concentration of enzyme was 0.13 μM (1.56 μM enzyme–flavin) and that of NAD^+ was 9.0 mM. The concentration of NADH ranged from 3.8–405 μM. An average of 13 determinations gave $K_{eq} = (1.0 \pm 0.1) \times 10^{-3}$. In the absorbance titration the concentration of enzyme complex was 0.37–0.91 μM (4.44–10.9 μM enzyme–flavin) and that of NAD^+ was 7.8–9.3 mM. The NADH concentration ranged from 4.3–81 μM. An average of 16 determinations gave $K_{eq} = (2.9 \pm 1.3) \times 10^{-3}$. Both of these numbers are only approximate as no corrections were made for possible alterations of the spectral properties and equilibrium constant caused by binding of NAD^+ and NADH to the enzyme.

Both NAD^+ and NADH were found to react very rapidly with the enzyme-bound flavin. When 0.37 μM enzyme complex in the standard buffer was mixed with 0.2 mM NADH in the standard buffer at 4 °C, the flavin reduction was over 95% complete within 5 ms, the dead time of the stopped-flow. Similarly, when 0.37 μM enzyme complex that was first reduced by incubation in deaerated standard buffer with 4 mM thiamin pyrophosphate, 2 mM $MgSO_4$, 1 mM pyruvate, 0.5 mM CoA, and 1 mM dithiothreitol on ice for 10 min was mixed with 3 mM NAD^+ at 4 °C, the flavin was at least 95% oxidized within the dead time of the instrument.

The relaxation time characterizing the interaction of NAD^+ and NADH with the enzyme-bound flavin was examined by the temperature-jump method using fluorescence detection. The solutions examined contained 0.36 μM enzyme complex (4.32 μM enzyme–flavin), 6 mM NAD^+, and 10.4–62 μM NADH in 0.1 M potassium phosphate (pH 7.0), and the final temperature was 16 °C. A single relaxation process was observed with a relaxation time of 19–24 μs. Since the rise time of the instrument is $\sim$10 μs, the relaxation time of the chemical process cannot be resolved; it must be $\leq$20 μs.

The reduction of the enzyme-bound flavin upon mixing the pyruvate dehydrogenase complex with thiamin pyrophosphate, $MgSO_4$, pyruvate, CoA, dithiothreitol, and NAD^+ in various concentrations and under various conditions in deaerated standard buffer at 4 °C was examined by fluorescence and absorbance measurements. Steady-state fluorescence emission spectra in Figure 2A show that the fluorescence emission at 520 nm (450-nm excitation) is quenched by 67% when 0.19 μM enzyme complex (2.28 μM enzyme–flavin) is incubated in 4 mM thiamin pyrophosphate, 2 mM $MgSO_4$, 5 mM pyruvate, 0.5 mM CoA, and 2 mM dithiothreitol (standard buffer, 4 °C). The absorption spectra in Figure 2B show that the extinction coefficient at 450 nm is decreased by 6% when 1.8 μM enzyme complex (21.6 μM enzyme–flavin) is incubated in 4 mM thiamin pyrophosphate, 2 mM $MgSO_4$, 4 mM pyruvate, 0.3 mM CoA, and 3 mM dithiothreitol (standard buffer, 4 °C). In both cases, doubling the substrate concentrations did not change the spectra further.

Stopped-flow experiments were carried out in the standard buffer of deaerated 0.02 M potassium phosphate, pH 7.0, at 4 °C. The specific activity of the enzyme complex was unaffected by passage through the stopped-flow system. The enzyme complex concentration after mixing was 0.18 μM in the fluorescence experiments and 0.32 μM in the absorbance experiments in most cases. When the enzyme complex was first incubated in the standard buffer with 4 mM thiamin pyrophosphate and 2 mM $MgSO_4$ on ice for at least 10 min and then mixed with the same buffer containing 1 mM CoA, 2 mM dithiothreitol, and varying amounts of pyruvate, changes in absorbance and fluorescence were observed in the time range of 5 ms–5 s. Typical kinetic traces are shown in part A (absorbance) and part B (fluorescence) of Figure 3. No changes in absorbance or fluorescence were observed in the absence of CoA.

The absorbance changes at 450 nm for all concentrations of pyruvate obeyed first-order kinetics and could be described by

$$y(\infty) - y(t) = A_1 e^{-k_1 t} \quad (7)$$

where $y(t)$ is the signal at time t, $y(\infty)$ is the signal at equilibrium, A_1 is an amplitude parameter, and k_1 is the first-order

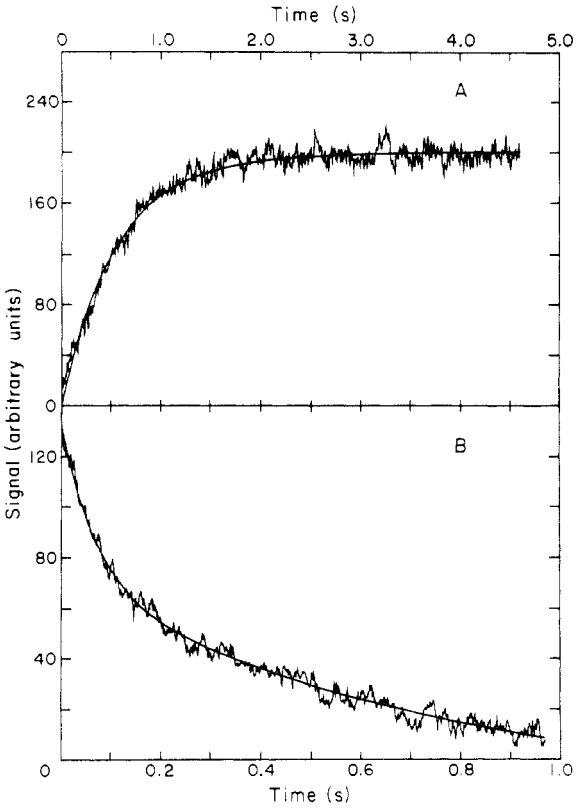

FIGURE 3: Typical kinetic traces for the reaction of pyruvate dehydrogenase complex incubated in 4 mM thiamin pyrophosphate, 2 mM $MgSO_4$, and 0.02 M potassium phosphate, pH 7.0, with pyruvate, CoA, and dithiothreitol in the same buffer at 4 °C. (A) Transmittance stopped-flow experiment with final concentrations of 0.32 μM enzyme complex (3.84 μM enzyme–flavin), 4 mM thiamin pyrophosphate, 2 mM $MgSO_4$, 0.87 mM pyruvate, 0.5 mM CoA, and 1 mM dithiothreitol. The wavelength used for observation was 450 nm. The trace shown represents an average of two oscilloscope traces. The solid line is the best fit to eq 7. (B) Fluorescence stopped-flow experiment with final concentrations of 0.18 μM enzyme complex (2.16 μM enzyme–flavin), 4 mM thiamin pyrophosphate, 2 mM $MgSO_4$, 0.77 mM pyruvate, 0.5 mM CoA, and 1 mM dithiothreitol. The excitation wavelength was 450 nm, and a 460-nm cutoff filter was inserted in front of the photomultiplier tube. The trace shown represents an average of two oscilloscope traces. The solid line is the best fit to eq 10.

rate constant of the reaction. The solid line in Figure 3A is the best fit to eq 7. The total signal change is 5.5–8%, as expected from the equilibrium measurements. At 3.6 mM pyruvate, the same rate constant was obtained over the wavelength range 440–480 nm. The range of final pyruvate concentrations was 0.017–3.6 mM. The results are summarized in Figure 4A as a plot of k_1 vs. the concentration of pyruvate. The simplest mechanism consistent with the data is a rapid equilibration of pyruvate with the enzyme complex (E) followed by an irreversible unimolecular reaction:

$$\text{E} + \text{pyruvate} \overset{K}{\rightleftharpoons} \text{E·pyruvate} \xrightarrow{k} \text{E·pyruvate}' \qquad (8)$$

The observed rate constant for this mechanism when the concentration of pyruvate is much greater than that of enzyme complex is

$$k_1 = \frac{k(\text{pyruvate})}{K + (\text{pyruvate})} \qquad (9)$$

where k is the rate constant of the second step and K is the equilibrium constant of the first step. Least-squares analysis of the data gives $k = 2.3\ s^{-1}$ and $K = 0.20$ mM; the curve in Figure 4A has been calculated with these parameters and eq 9.

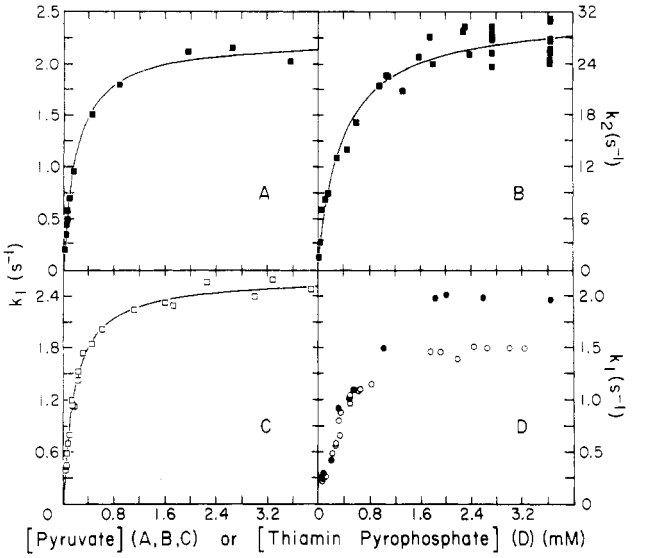

FIGURE 4: Plots of rate constants k_1 and k_2 vs. concentration of pyruvate (A, B, and C) or thiamin pyrophosphate (D), where k_1 is defined by eq 7 (A and D) or eq 10 (C) and k_2 is defined by eq 10 (B). The three lines were calculated with eq 9: (A) $k = 2.3\ s^{-1}$ and $K = 0.20$ mM; (B) $k = 29.7\ s^{-1}$ and $K = 0.37$ mM; (C) $k = 2.6\ s^{-1}$ and $K = 0.17$ mM. The data in (A–C) were obtained in 4 mM thiamin pyrophosphate, 2 mM $MgSO_4$, 0.5 mM CoA, 1 mM dithiothreitol, and 0.02 M potassium phosphate, pH 7.0, at 4 °C with 0.073–0.46 μM enzyme complex. In (D) the data were obtained in 2 mM $MgSO_4$, 3 mM pyruvate, 0.3–0.7 mM CoA, 3–7 mM dithiothreitol, and 0.02 M potassium phosphate, pH 7.0, at 4 °C by following changes in absorbance (○) at 450 nm and fluorescence (●) with excitation at 450 nm and a 460-nm cutoff filter for the emission.

The fluorescence changes could not be described well by eq 7. However, the assumption of two first-order kinetic processes fits the data well. Accordingly, the kinetic traces were fit to the equation

$$y(t) - y(\infty) = A_1 e^{-k_1 t} + A_2 e^{-k_2 t} \qquad (10)$$

where the variables have definitions analogous to those in eq 7. The solid line in Figure 3B is the best fit to eq 10. The total signal change at 450-nm excitation was 60–65%, again in reasonable agreement with the equilibrium measurements. Because in most cases k_1 was less than one-tenth k_2, both rate constants could not be precisely determined from the same kinetic traces. Therefore, two sets of experiments over different time ranges were used to obtain the rate constants. The rate constants for the faster process, k_2 (Figure 4B), were obtained over a final pyruvate concentration range of 0.020–3.67 mM. The rate constants for the slower process, k_1 (Figure 4C), were obtained over a final pyruvate concentration range of 0.024–3.80 mM. The dependence of the rate constants on the concentration of pyruvate conforms well to eq 9. The best-fit parameters to eq 9 obtained from least-squares analysis gives $k = 29.7\ s^{-1}$, $K = 0.37$ mM (k_2) and $k = 2.6\ s^{-1}$, $K = 0.17$ mM (k_1). The curves in parts B and C of Figure 4 have been calculated with these parameters and eq 9. The relative amplitudes of the two processes, A_1 and A_2, did not vary with pyruvate concentration and $A_1/A_2 = 0.85$.

The rate constants and amplitudes obtained from the fluorescence measurements were not significantly altered over the range of 0.073–0.46 μM enzyme complex when enzyme complex incubated in 4 mM thiamin pyrophosphate and 2 mM $MgSO_4$ was mixed with 4 mM thiamin pyrophosphate, 2 mM $MgSO_4$, 6 mM pyruvate, 1 mM CoA, and 2 mM dithiothreitol (all in standard buffer at 4 °C). Similarly, the first-order rate constants and the amplitudes did not vary over a concentration range of 5.8 μM–1 mM CoA in the absorbance and fluores-

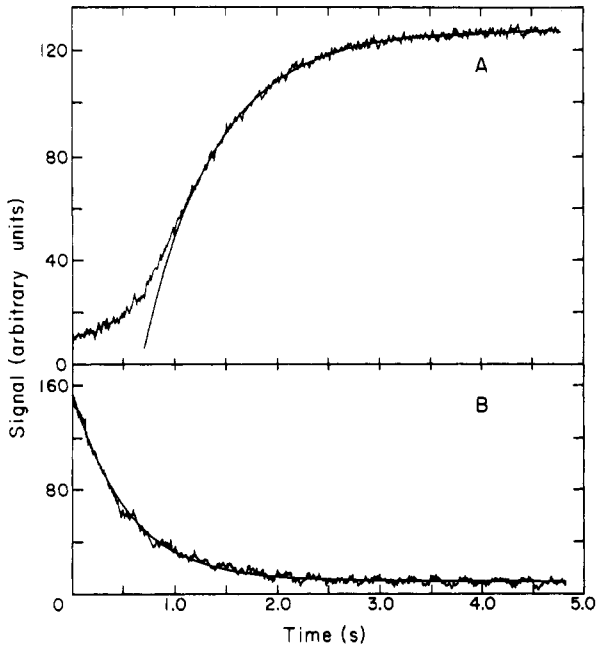

FIGURE 5: Typical kinetic traces for reaction of pyruvate dehydrogenase complex with thiamin pyrophosphate, $MgSO_4$, pyruvate, CoA, and dithiothreitol in 0.02 M potassium phosphate, pH 7.0, at 4 °C. (A) Transmittance stopped-flow experiment with final concentrations of 0.32 μM enzyme complex (3.84 μM enzyme–flavin), 4.1 mM thiamin pyrophosphate, 4 mM $MgSO_4$, 3 mM pyruvate, 0.7 mM CoA, and 3 mM dithiothreitol. The wavelength used for observation was 450 nm. The trace shown represents an average of three oscilloscope traces. The solid line is the best fit to eq 7. (B) Fluorescence stopped-flow experiment with final concentrations of 0.18 μM enzyme complex (21.6 μM enzyme–flavin), 3.6 mM thiamin pyrophosphate, 2 mM $MgSO_4$, 3 mM pyruvate, 0.5 mM CoA, and 1 mM dithiothreitol. The excitation wavelength was 450 nm, and a 460-nm cutoff filter was inserted in front of the photomultiplier tube. The trace shown represents an average of two oscilloscope traces. The solid line is the best fit to eq 10.

cence kinetic measurements. The reduced enzyme obtained after mixing the reactants in the stopped flow was fully active. When the complex is incubated with 4 mM thiamin pyrophosphate and 2 mM $MgSO_4$ and mixed with 4 mM thiamin pyrophosphate, 2 mM $MgSO_4$, 2 mM dithiothreitol, 5 mM pyruvate, CoA, and NAD^+ in standard buffer at 4 °C, the rate constants are unchanged over a range of NAD^+ concentrations from 0 to 6 mM at CoA concentrations of 1 and 6.4 mM.

If the reaction was monitored by absorbance changes at 530 nm in the stopped-flow measurements, a biphasic time course was observed: a rapid increase in absorbance was followed by a relatively slow decrease. The first-order rate constants correspond to those obtained by monitoring fluorescence. If the total absorbance was ~0.04 at 530 nm, the total increase corresponds to an absorbance of 0.02 and the total decrease to an absorbance of 0.01, with a resulting net increase in absorbance of ~0.01.

If the enzyme complex is not incubated with thiamin pyrophosphate and $MgSO_4$ before mixing it with the substrates, both the absorbance and fluorescence kinetic traces are altered. When the enzyme complex is mixed with 0.6–1.4 mM CoA, 6–14 mM dithiothreitol, 6 mM pyruvate, 4 mM $MgSO_4$, and varying concentrations of thiamin pyrophosphate in the standard buffer at 4 °C, a slow change in absorbance occurs followed by a more rapid change. Only the latter, more rapid, change can be described by eq 7. This is illustrated in Figure 5A where the solid line is calculated with eq 7. The induction time before the onset of first-order behavior ranged from 680 to 3380 ms and decreased with increasing thiamin pyrophosphate concentrations (0.03–4.1 mM). The first-order rate constants obtained are plotted vs. the final concentration of thiamin pyrophosphate in Figure 4D. The fluorescence kinetic traces were obtained by mixing the enzyme complex with 1 mM CoA, 2 mM dithiothreitol, 6 mM pyruvate, 2 mM $MgSO_4$ and varying concentrations of thiamin pyrophosphate in the standard buffer at 4 °C. A typical kinetic trace is shown in Figure 5B. Most of the time courses can be described by a single exponential function (eq 7) and no significant induction period occurs. The first-order rate constants are included in Figure 4D. At high concentrations of thiamin pyrophosphate (>2 mM), the time course of fluorescence changes is better described by two first-order rate processes (eq 10) although the resolution is poor because k_1 and k_2 are similar in magnitude. The first-order rate constants from both the absorbance and fluorescence measurements reach a limiting value of 1.5–2.0 s^{-1}. The simplest interpretation for these data is that a conformational change triggered by the binding of thiamin pyrophosphate is rate limiting in lipoic acid oxidation when the enzyme complex is not incubated with thiamin pyrophosphate before mixing with the other substrates.

When enzyme complex incubated with 4 mM thiamin pyrophosphate, 2 mM $MgSO_4$, and 0.11–1.3 mM oxaloacetate is mixed with 0.6 mM CoA, 4 mM dithiothreitol, 6.4 mM pyruvate, and 0.11–1.3 mM oxaloacetate in the standard buffer at 4 °C, the rate constant of the slower process and the relative amplitudes are not altered by the presence of oxaloacetate, but the rate constant of the faster process was increased to 41 ± 3 s^{-1}. The effect of oxaloacetate on the rate of acetylation was studied by the quenched-flow method: 0.32 μM enzyme complex incubated with 4 mM thiamin pyrophosphate, 2 mM $MgSO_4$, and 0.23 mM oxaloacetate was mixed with 4.4 mM pyruvate, 4 mM thiamin pyrophosphate, 2 mM $MgSO_4$, and 0.23 mM oxaloacetate in the standard buffer at 4 °C; the time course of acetylation from 0.03 to 3 s was observed. As previously described (Akiyama & Hammes, 1980), the time course of acetylation can be described as a sum of two first-order rate processes

$$y = A_1e^{-k_1t} + (1 - A_1)e^{-k_2t}$$

where y is now the fraction of unreacted enzyme, k_1 and k_2 are first-order rate constants, and A_1 is an amplitude parameter. The rate constants obtained were $k_1 = 50.9\ s^{-1}$, $k_2 = 0.78\ s^{-1}$, and $A_1 = 0.55$. In the absence of oxaloacetate, $k_1 = 25.4\ s^{-1}$, $k_2 = 0.97\ s^{-1}$, and $A_1 = 0.58$. Thus, oxaloacetate specifically increases the rate constant for catalytic acetylation (k_1).

The steady-state kinetics of NADH formation was also studied in the stopped flow by observing the formation of NADH at 340 nm. When 0.15 μM enzyme complex incubated with 4 mM thiamin pyrophosphate and 4 mM $MgSO_4$ is mixed with 4 mM thiamin pyrophosphate, 4 mM $MgSO_4$, 6 mM pyruvate, 1.0 mM CoA, 1 mM dithiothreitol, and 6 mM NAD^+ in standard buffer at 4 °C, the change in the 340-nm transmittance with time becomes linear with an exponential time constant of ~30 ms.

Discussion

The titration of the enzyme with NADH in the presence of NAD^+ results in the formation of the two-electron reduced lipoamide dehydrogenase which is predominantly a charge-transfer complex between a reduced disulfide and oxidized flavin (Massey & Veeger, 1961; Williams, 1965, 1975; Matthews et al., 1977). The discrepancy between the equilibrium constants obtained from the fluorescence (K_{eq} = 1.0

$\times 10^{-3}$) and the absorbance ($K_{eq} = 2.9 \times 10^{-3}$) titrations can be attributed to several factors. In the absorbance titrations, the precision is diminished by the difficulty in obtaining a proper blank correction. The small absorbance changes could not be corrected precisely for the amount of NADH which was added and subsequently oxidized to NAD^+ and for NADH bound to the enzyme. The absence of well-defined isosbestic points in the spectra in Figure 1B may indicate the occurrence of multiple equilibria but is more likely an artifact due to inexact blank corrections. Titrations of pig heart lipoamide dehydrogenase with NADH, both in the presence of NAD^+ (Williams, 1975) and in the absence of NAD^+ (Massey & Veeger, 1961) did not yield well-defined isosbestic points, but spectra of isolated lipoamide dehydrogenase from *E. coli* reduced with dithionite showed isosbestic points at 503, 436, 387, and 336 nm (Wilkenson & Williams, 1979). Although a double-reciprocal plot of $1/\Delta F$ vs. $1/[NADH]$ is linear (not shown), the fluorescence changes probably contain contributions from the binding of NAD^+ and NADH to the enzyme complex which may have altered the calculated equilibrium constant. Comparison of the fluorescence emission spectra in Figures 1A and 2A shows that whereas reduction of the flavin by thiamin pyrophosphate, Mg^{2+}, pyruvate, and CoA causes 65% fluorescence quenching, reduction by NADH causes 97% quenching. The increased quenching after reduction by NADH may be due to bound NADH or to formation of the four-electron reduced enzyme. Previous reports have shown NADH reduction to cause an 85–100% quenching of flavin fluorescence, and dithionite reduction to the two-electron reduced enzyme resulted in 77–80% quenching of the flavin fluorescence in the isolated *E. coli* lipoamide dehydrogenase and 86–91% quenching in the corresponding pig heart enzyme (Wilkenson & Williams, 1979).

The spectrum in Figure 2B suggests that the predominant product of mixing thiamin pyrophosphate, Mg^{2+}, pyruvate, and CoA with the enzyme complex is the two-electron reduced form of lipoamide dehydrogenase (Williams, 1975). The four-electron reduced form has been obtained under completely anaerobic conditions (Frey et al., 1978). However, the reduced enzyme obtained in this work can be further reduced by the addition of NADH.

The stopped-flow experiments reveal the occurrence of at least two kinetic processes. The faster process can be observed by monitoring changes in the absorbance at 530 nm and in the fluorescence emission. Only this process has a sufficiently high rate to be catalytically significant. The limiting first-order rate constant is 30 s^{-1} at high pyruvate concentrations. This is similar to the overall turnover number of 35 s^{-1} which is obtained if 12 pyruvate decarboxylases are assumed to be coupled into the catalytic cycle and to the maximum rate constant for acetylation (45–60 s^{-1}; Akiyama & Hammes, 1980). The dependence of the faster process on the concentration of pyruvate yielded an equilibrium dissociation constant for the binding of pyruvate to the enzyme complex of 0.37 mM, in good agreement with the values obtained from direct binding measurements (0.31 mM; Shepherd & Hammes, 1976) and from the dependence of the rate of acetylation on the pyruvate concentration (0.47 mM; Akiyama & Hammes, 1980). Incubation of the enzyme with oxaloacetate specifically increases the rate of the faster process by a factor of 1.5. Since oxaloacetate also specifically increases the rate of catalytic acetylation of the lipoic acids by a factor of 2.0, this suggests that the rate-determining step for the faster process observed in the stopped-flow experiments can be assigned to a step in catalytic acetylation.

The slower process, which can be monitored by either fluorescence or absorbance changes at 450 and 530 nm, is too slow to be catalytically significant. The limiting rate constant is 2.3–2.6 s^{-1} at high pyruvate concentrations which is much slower than the minimum turnover number of 17.5 s^{-1} obtained if 24 pyruvate decarboxylases are assumed to participate in the catalytic cycle (Akiyama & Hammes, 1980). Furthermore, the catalytic steady state is established more rapidly than allowed by the rate of the slower step. The dependence of the slower rate constants on the pyruvate concentration gave an equilibrium dissociation constant of 0.17–0.20 mM for pyruvate binding to the enzyme if the model in eq 8 is assumed.

A mechanistic explanation of the observed results is that the faster process corresponds to formation of the catalytically active two-electron reduced enzyme, while the slower process represents subsequent partial conversion of the two-electron reduced species to the catalytically inactive four-electron reduced species. This is consistent with the observed fluorescence changes, with the absorption changes at 530 nm, and with the fact that the enzyme can be further reduced. However, results obtained with the pig heart lipoamide dehydrogenase suggest that a decrease in the absorbance at 450 nm also should be associated with the faster process (Williams, 1975), and this is not observed. Computer modeling of the time courses obtained at 450 nm indicates that either no change or an increase in absorbance at 450 nm could be associated with the rapid process, but a decrease in absorbance cannot be accommodated by the data. Apparently, this represents a difference in the spectral properties of the two-electron reduced lipoamide dehydrogenase free and in the multienzyme complex.

The dependence of k_2, the rate of catalytic acetylation, on the pyruvate concentration requires the rate-determining step of the mechanism shown in eq 1–5 to be the first irreversible step; this is most probably the decarboxylation of pyruvate and the concomitant formation of the hydroxyethylthiamin pyrophosphate complex. The rate of flavin reduction is independent of the concentration of CoA used, indicating the rate of deacetylation of the lipoic acids by CoA is much faster than the rate of acetylation. These conclusions are in agreement with those reached from a quenched-flow study of lipoic acid acetylation (Akiyama & Hammes, 1980).

The mechanism of action of the pyruvate dehydrogenase multienzyme complex is not simple because more than one pathway for acetylation and flavin reduction exists. Not all of the lipoic acids and flavins are necessary for catalysis (Angelides & Hammes, 1978; Collins & Reed, 1977; Ambrose-Griffin et al., 1980). The role of these multiple pathways in the catalytic mechanism is not clear. The simplest mechanism consistent with all of the results is that acetyl groups and electrons can shuttle rapidly between lipoic acids during catalysis with the reaction catalyzed by pyruvate decarboxylase being rate determining in the catalytic cycle.

References

Akiyama, S. K. (1981) Ph.D. Thesis, Cornell University, Ithaca, NY.

Akiyama, S. K., & Hammes, G. G. (1980) *Biochemistry 19*, 4208.

Ambrose-Griffin, M. C., Danson, M. J., Griffin, W. G., Hale, G., & Perham, R. N. (1980) *Biochem. J. 187*, 393–401.

Angelides, K. J., & Hammes, G. G. (1978) *Proc. Natl. Acad. Sci. U.S.A. 75*, 4877–4880.

Angelides, K. J., & Hammes, G. G. (1979) *Biochemistry 18*, 1223–1229.

Angelides, K. J., Akiyama, S. K., & Hammes, G. G. (1979) *Proc. Natl. Acad. Sci. U.S.A. 76*, 3279–3283.

Bates, D. L., Danson, M. J., Hale, G., Hooper, E. A., & Perham, R. N. (1977) *Nature (London) 268*, 313–316.
Brown, J. P., & Perham, R. N. (1976) *Biochem. J. 155*, 419–427.
Collins, J. H., & Reed, L. J. (1977) *Proc. Natl. Acad. Sci. U.S.A. 74*, 4223–4227.
del Rosario, E. J. (1970) Ph.D. Thesis, Cornell University, Ithaca, NY.
Fersht, A. R., & Jakes, R. (1975) *Biochemistry 14*, 3350–3356.
Frey, P. A., Ikeda, B. H., Gavino, G. R., Speckhard, D. C., & Wong, S. S. (1978) *J. Biol. Chem. 253*, 7234–7241.
Hilborn, D. A. (1972) Ph.D. Thesis, Cornell University, Ithaca, NY.
Hilborn, D. A., Harrison, L. W., & Hammes, G. G. (1973) *Comput. Biomed. Res. 6*, 216–227.
Koike, M., & Reed, L. J. (1960) *J. Biol. Chem. 235*, 1924–1930.
Koike, M., Reed, L. J., & Carroll, W. R. (1963) *J. Biol. Chem. 238*, 30–39.
Lowry, O. H., Rosebrough, N. J., Farr, A. L., & Randall, R. J. (1951) *J. Biol. Chem. 193*, 265–275.
Lymn, R. W., & Taylor, E. W. (1970) *Biochemistry 9*, 2975–2983.
Massey, V., & Veeger, C. (1961) *Biochim. Biophys. Acta 48*, 33–47.
Matthews, R. G., Ballou, D. P., Thorpe, C., & Williams, C. H. (1977) *J. Biol. Chem. 252*, 3199–3207.
Meister, A. (1950) *J. Biol. Chem. 184*, 117–129.
Reed, L. J. (1974) *Acc. Chem. Res. 7*, 40–46.
Reed, L. J., & Willms, C. R. (1966) *Methods Enzymol. 9*, 246–265.
Shepherd, G. B., & Hammes, G. G. (1976) *Biochemistry 15*, 311–317.
Shepherd, G. B., & Hammes, G. G. (1977) *Biochemistry 16*, 5234–5240.
Speckhard, D. C., Ikeda, B. H., Wong, S. S., & Frey, P. A. (1977) *Biochem. Biophys. Res. Commun. 77*, 708–713.
Wilkenson, K. D., & Williams, C. H. (1979) *J. Biol. Chem. 254*, 852–862.
Williams, C. H. (1965) *J. Biol. Chem. 240*, 4793–4800.
Williams, C. H. (1975) *Enzymes, 3rd Ed.* 13, 89–173.
Willms, C. R., Oliver, R. M., Henry, H. R., Mukherjee, B. B., & Reed, L. J. (1967) *J. Biol. Chem. 242*, 889–897.

Purification and Properties of Mouse Pyruvate Kinases K and M and of a Modified K Subunit†

Kenneth H. Ibsen,* Robert H.-C. Chiu,‡ Hae Ryun Park, Dennis A. Sanders, Srecko Roy, Kirk N. Garratt, and Mark K. Mueller

ABSTRACT: The K_4 and M_4 isozymes of mouse pyruvate kinase were purified to homogeneity, and their physical, chemical, and kinetic properties were compared. The K isozyme is slightly larger, but a high degree of homology exists as evidenced by a similar amino acid composition, immunotitration value, and two-dimensional arginine peptide pattern after tryptic digestion. Also, the more active conformational form of the K isozyme has kinetic and chromatographic properties similar to those of the M isozyme. Only K subunit could be extracted with antibody from fresh spleen extracts, but this subunit can be cleaved to form a product with the mobility of the M subunit. The cleavage is accomplished by an endogenous enzyme and appears to be the first step in K-enzyme degradation. This product is called K^{pm}. $K^{pm}K$ hybrid could also be purified to homogeneity. This enzyme has the structure $K_2^{pm}K_2$, and both types of subunit have activity. The K^{pm} form has a higher $K_{0.5S}$ value for phosphoenolpyruvate and a lower $K_{0.5S}$ value for ADP than does either the K or the M type. However, the K^{pm} and M subunits otherwise have very similar properties and it is speculated that the K^{pm} subunit is an M-type precursor.

Four tissue-specific types of pyruvate kinase subunits have been identified. Immunologic criteria divide these into two non-cross-reacting groups: the L and L′ types and the M and K types[1] [see Hall & Cottam (1978) for review]. The L and L′ subunits also have a simlar amino acid composition [see Hall & Cottam (1978)] and yield similar fingerprint patterns (Saheki et al., 1978), and the L subunit has been reported to be formed from the L′ type by proteolysis (Marie et al., 1977). Thus these two forms are probably products of a single gene. The K and M types also have antigenic determinants in common, and the K type has been reported to be converted to the M type (Marie et al., 1976). However, they have also been reported to have very different peptide fingerprint patterns (Saheki et al., 1978), and comparative amino acid composition

† From the Department of Biological Chemistry, California College of Medicine, University of California, Irvine, Irvine, California 92717. *Received July 8, 1980.* Phases of this investigation were supported by U.S. Public Health Service Grant CA-07883-12 and grants from the American Diabetes Association, the Institutional Biomedical Research Support Grant-Fund (23876), and the University of California Cancer Research Coordinating Committee. Portions of this work were reported in abstract form (Wilson & Ibsen, 1976; Ibsen et al., 1980).

‡ Present address: Department of Molecular Biology, University of Southern California, Los Angeles, CA 90007.

[1] In this investigation the L, K, M nomenclature will be used, with subscripts to identify the quarternary structure when relevant. The homotetrameric K_4 enzyme is also commonly called the M_2 or A isozyme. The L′ subunit is found in red blood cells, and the native isozyme is often called the R or D isozyme [see Ibsen (1977) for review]. The subunit derived from the K form having a mobility like the M subunit is called K^{pm}, i.e., the K subunit pseudo-M-type product.

0006-2960/81/0420-1497$01.25/0